



Contents lists available at ScienceDirect

Saudi Pharmaceutical Journal

journal homepage: www.sciencedirect.com



Original article

## Molecular interaction of tea catechin with bovine $\beta$ -lactoglobulin: A spectroscopic and in silico studies

Nasser Abdulatif Al-Shabib <sup>a,1,\*</sup>, Javed Masood Khan <sup>a,1</sup>, Ajamaluddin Malik <sup>b</sup>, Md. Tabish Rehman <sup>c</sup>, Mohamed F. AlAjmi <sup>c</sup>, Fohad Mabood Husain <sup>a</sup>, Malik Hisamuddin <sup>d</sup>, Nojood Altwaijry <sup>b</sup>

<sup>a</sup> Department of Food Science and Nutrition, Faculty of Food and Agricultural Sciences, King Saud University, 2460, Riyadh 11451, Saudi Arabia

<sup>b</sup> Protein Research Chair, Department of Biochemistry, College of Science, King Saud University, Riyadh, Saudi Arabia

<sup>c</sup> King Saud University, Department of Pharmacognosy, College of Pharmacy, Riyadh 11451, Saudi Arabia

<sup>d</sup> Centre for Interdisciplinary Research in Basic Sciences, Jamia Millia Islamia, New Delhi, India

### ARTICLE INFO

#### Article history:

Received 20 August 2019

Accepted 19 January 2020

Available online 27 January 2020

#### Keywords:

Polyphenol

Catechin

Beta-Lactoglobulin

Protein and proteinligand, interaction

### ABSTRACT

Polyphenols have attained pronounced attention due to their beneficial values of health and found to prevent several chronic diseases. Here, we elucidated binding mechanism between frequently consumed polyphenol "tea catechin" and milk protein bovine beta-lactoglobulin ( $\beta$ -Lg). We investigated the conformational changes of  $\beta$ -Lg due to interaction with catechin using spectroscopic and in silico studies. Fluorescence quenching data (Stern-Volmer quenching constant) revealed that  $\beta$ -Lg interacted with catechin via dynamic quenching. Thermodynamic data revealed that the interaction between  $\beta$ -Lg and catechin is endothermic and spontaneously interacted mainly through hydrophobic interactions. The UV-Vis absorption and far-UV circular dichroism (CD) spectroscopy exhibited that the tertiary as well as secondary structure of  $\beta$ -Lg distorted after interaction with catechin. Molecular docking and simulation studies also confirm that catechin binds at the central cavity of  $\beta$ -Lg with high affinity ( $\sim 10^5$  M<sup>-1</sup>) and hydrophobic interactions play significant role in the formation of a stable  $\beta$ -Lg-catechin complex.

© 2020 The Author(s). Published by Elsevier B.V. on behalf of King Saud University. This is an open access article under the CC BY-NC-ND license (<http://creativecommons.org/licenses/by-nc-nd/4.0/>).

## 1. Introduction

Tea is a very popular drink beverage worldwide (Graham, 1992). Tea contains different types of flavonoids which are generally polyphenols. Tea polyphenol is also called as catechins. Several types of catechins were found such as (–)-epicatechin (EC), (–)-epicatechin-3-gallate, (–) epigallocatechin-3-gallate and ellagic acid (Naghma and Hasan, 2019). Tea polyphenols also have antioxidant as well as anticancer properties, and hence known as important chemo preventive products (Dreostic et al., 1997). Indeed, the intake of polyphenols has been linked with a reduced risk of stroke, cancers and coronary heart disease (Shah et al., 2010; Du et al., 2013). The tea polyphenols can reduce carcinogenesis in human

by scavenging the production of reactive oxygen species (ROS) (Mao et al., 2019). In spite of beneficial effects, it is also reported that polyphenol causes harmful effects, particularly when consumed at high concentrations (Arts et al., 2001). It will be interesting to see the interactions between the polyphenols and biomolecules, which are found in the human body, like proteins and lipids (Nozaki et al., 2009). Moreover, complete understanding of protein and polyphenol interaction is still lacking. It was reported that polyphenol interacted with different proteins including serum albumin from bovine and human origin (Dufour and Dangles, 2005). The rice gluten interacted with epigallocatechin-3-gallate (EGCG) and form complexes which might significantly affect physicochemical properties of gluten (Xu et al., 2019). Ellagic acids is a polyphenol found in tea, pomegranate, strawberry, and walnut and binds with bovine serum albumin through electrostatic interaction (Fengru et al., 2019). Protein and polyphenol interaction give more insight into our current understanding of polyphenols induces conformational changes under physiological conditions.

Several transporter proteins are known which can bind with variety of ligand or drugs (Tantimongcolwat et al., 2019; Shen et al., 2013). Among the transporter, protein bovine  $\beta$ -

\* Corresponding author.

E-mail address: [nalshabib@ksu.edu.sa](mailto:nalshabib@ksu.edu.sa) (N.A. Al-Shabib).

<sup>1</sup> Authors are equally contributed.

Peer review under responsibility of King Saud University.



lactoglobulin ( $\beta$ -Lg) is one of the good transporter protein, which is usually transport hydrophobic ligand efficiently (Al-Shabib et al., 2018).  $\beta$ -Lg is a globular transporter protein of 18.3 kDa mass and comprises of 162 amino acids residues (Patel et al., 2019). The nuclear magnetic resonance (NMR) spectroscopy and X-ray crystallography data revealed that the  $\beta$ -Lg exist in monomer at acidic pH and dimer at neutral pH (Uhrinova et al., 2000; Qin et al., 1999). The folded monomer of  $\beta$ -Lg contains eight stranded antiparallel  $\beta$ -sheets, which are involved in the formation of hydrophobic pocket or calyx (Monaco et al., 1987).  $\beta$ -Lg is highly used in the food and pharmaceutical industries because of its capability to bind vitamins fatty acids, and several other ligands (Ragona et al., 2000).  $\beta$ -Lg has two binding sites for hydrophobic molecules, one at inside the calyx and other one is at the dimer interface. Another binding site was also reported called as site B. From the fluorescence measurements, it was noted that retinoids and fatty acids interact independently; retinoids binds at the central cavity of  $\beta$ -Lg while fatty acids interacted at the external site (Creamer, 1995). Based on fluorescence resonance energy transfer techniques, it was characterized that some ligands like retinol, retinoic acid and bis-ANS bind at the surface of  $\beta$ -Lg rather than at the internal cavity of calyx (Lange et al., 1998). Interaction of milk protein with phenolic compound, which is found in food, is investigated in details (Zhang et al., 2014). It was also reported that the tea polyphenol affects the antioxidant property of  $\alpha$ -lactalbumin protein due covalent interaction with  $\alpha$ -lactalbumin (Almajano et al., 2007).  $\beta$ -Lg interaction with several polyphenols (chlorogenic acid (CGA), epigallocatechin-3-gallate (EGCG) and ferulic acid (FA)) was characterized and concluded that EGCG had more binding affinity with  $\beta$ -Lg than other two polyphenols (Jia et al., 2017).

In previous studies, it was reported that the proteins and polyphenols form complexation due to non-covalent interaction, which stabilized the protein confirmation (Chaudhuri et al., 2011; Kanakis et al., 2011). Few researchers reported that the proteolytic digestion was decreased due to complexations of polyphenols and  $\beta$ -Lg and this complexation reduces the free radical scavenging property (Stojadinovic et al., 2013). Nevertheless, the detail interaction mechanism between  $\beta$ -Lg and tea polyphenol i.e., catechin is not studied. Consequently, the aim of this work was to examine the mechanism of interaction between  $\beta$ -Lg and tea catechin polyphenol at physiological pH. To decipher the mechanism, we have used multi spectroscopic (ultraviolet–visible (UV) absorption, fluorescence quenching and circular dichroism (CD) spectroscopy) and computational (molecular docking and simulation) techniques. The above biophysical techniques are highly utilized to characterize the protein–ligand interactions (Yadav et al., 2018a, 2018b). Molecular dynamic simulation is very good computational techniques to use to understand macromolecular structure–to–function relationships (Yadav et al., 2016). The obtained results of this study proposed the mechanism of interaction of  $\beta$ -Lg and catechin in food and pharma industries.

## 2. Materials and methods

The  $\beta$ -Lg and (+)-catechin hydrate was purchased from the Sigma Chemical Company (St. Louis, MO, USA). The other reagents were used in this articles are analytical grade.

### 2.1. Solution preparations

All the spectroscopic measurements were performed in 20 mM sodium phosphate buffer, pH 7.4.  $\beta$ -Lg was dissolved in same buffer and dialyzed for four hours in sodium phosphate buffer pH 7.4. Dialyzed  $\beta$ -Lg was further filtered through 0.22- $\mu$ m Millipore syringe

filter. After filtration,  $\beta$ -Lg stock concentration was calculated according to already reported method (Al-Shabib et al., 2018). The tea catechin was dissolved in 5.0 ml of MilliQ water.

### 2.2. UV–Vis absorption spectroscopy

The absorption spectra were collected on Agilent Technologies Carry 60 spectrophotometer.  $\beta$ -Lg (11.0  $\mu$ M) was incubated without and with different concentrations of catechin (0–100  $\mu$ M) at room temperature. The incubated samples were scanned in quartz cuvette. The blank of phosphate buffer without catechin and with catechin was also scanned and subtracted from the working samples. The UV-Visible spectra of incubated and blank samples were scanned in the range of 200–450 nm at room temperature.

### 2.3. Fluorescence spectroscopy

Fluorescence is very valuable technique to examine interactions between  $\beta$ -Lg and catechin. Intrinsic fluorescence was investigated at three different temperatures (288, 298, and 310 K) on Agilent Technologies Carry Eclipse fluorescence spectrophotometer equipped with peltier thermostatted multicell holder. The samples in 1.0 cm path-length quartz cell were excited at 295 nm and emission was recorded in the range of 300–450 nm and excitation and emission slit widths were fixed at 5.0 nm. The fixed  $\beta$ -Lg concentration (2.0  $\mu$ M) was used in all the samples. The catechin (0–7.5  $\mu$ M) was added stepwise manner in a 3.0 ml quartz cuvette. The stock concentration of catechin was 500  $\mu$ M and every titration 2.0  $\mu$ l of catechin was added. The details of data analysis was provided in supplementary methods in [supplementary data](#) as a SMI.

### 2.4. Far-UV circular dichroism (CD)

Far-UV CD spectra of  $\beta$ -Lg with and without catechin complexes were studied with Chirascan Plus, spectropolarimeter (Applied Photophysics). For far-UV CD measurements, a quartz cell with a path length of 0.1 cm was used in continuous nitrogen flushing.  $\beta$ -Lg concentration was taken (0.2 mg.ml<sup>-1</sup>), while different concentrations (10.0, 50.0 and 100.0  $\mu$ M) of catechin were taken. Every sample was scan twice. The spectra were collected at room temperature from 250 to 200 nm at the interval of 1.0 nm.

### 2.5. Molecular docking and simulation studies

Interaction between  $\beta$ -Lg (PDB ID:4Y0P; 2.20 Å resolution) (Loch et al., 2015) and catechin (PubChem ID: 9064) was reviewed by performing molecular docking and molecular dynamics simulation using different modules of Schrodinger suite in Maestro (Schrödinger, LLC, NY, USA) as described previously (Rehman et al., 2019; AlAjmi et al., 2018). Briefly, the structure of catechin was drawn in 2D sketcher and prepared for docking using LigPrep (Schrödinger, LLC, NY, USA). All the possible conformations of catechin were generated at pH 7.0  $\pm$  2.0 using Epik (Schrödinger, LLC, NY, USA) and energy minimized with the help of OPLS3e forcefield. Protein ( $\beta$ -Lg) was optimized for docking using Glide (Schrödinger, LLC, NY, USA) by removing non-essential water molecules, adding hydrogen atoms, generating any missing side chains and loops using Prime (Schrödinger, LLC, NY, USA) and removing any other heterogenous molecule. Grids map was generated by selecting the ligand (tetracaine) which was bound in the X-ray structure as the center of grid box. The size of grid box for  $\beta$ -Lg was 72  $\times$  72  $\times$  72 Å. Molecular docking was performed with extra-precision (XP) modes in Glide (Schrödinger, LLC, NY, USA) keeping all the parameters at default values.

Desmond (Schrödinger, LLC, NY, USA) was employed to perform molecular dynamics simulation for 50 ns at 300 K and 1 bar pres-

sure (Kumar et al., 2018; Yadav et al., 2018a,2018b). The simulation was performed inside an orthorhombic box the boundaries of which were at least 10 Å away from the protein. The simulation box was solvated using TIP3P explicit solvent model and the whole system was neutralized by adding adequate counterions. The physiological conditions were mimicked by adding 150 mM NaCl to the simulation box. Finally, OPLS3e forcefield was employed to energy-minimize the system till it converges to 1 kcal/mol/Å.

### 3. Results and discussion

#### 3.1. Steady state fluorescence quenching measurements

Fluorescence quenching was generally used to identify the protein–ligand interaction (Alanazi et al., 2019). The fluorophores of proteins are proteins (tryptophan, tyrosine, and phenylalanine) are sensitive to their microenvironment and hence can be used to studying ligand-induced conformational changes. The quenching in fluorescence takes place only if a ligand binds to a protein and affects the emission of intrinsic fluorophores. The  $\beta$ -Lg has two (Trp) residues at position of 19 and 61 (Wu et al., 2013). Therefore, Trp fluorescence quenching of  $\beta$ -Lg without and with catechin was performed. The fluorescence intensities of  $\beta$ -Lg at pH 7.4 without and with catechin at three temperatures (288, 298 and 310 K) after excitation of 295 nm have been shown in Fig. 1A–C. From the figs., it can be clearly seen that the  $\beta$ -Lg without catechin showed maximum fluorescence at  $\sim$  337 nm which is similar to other published reports (Jia et al., 2017). The fluorescence intensity of  $\beta$ -Lg without catechin was found to decrease at higher temperatures (288  $\geq$  298  $\geq$  310 K). After that we have gradually added catechin to  $\beta$ -Lg samples at 288, 298 and 310 K. The fluorescence intensity of  $\beta$ -Lg continuously decreased with slightly red shift in wavelength maximum, which is shown in Fig. 1A–C. The regular decrease in  $\beta$ -Lg fluorescence intensity and shift in wavelength maxima confirms that the catechin binds with  $\beta$ -Lg and causes conformational changes in  $\beta$ -Lg protein. The quenching mechanism was further investigated. Fluorescence quenching between ligand and protein takes place via two mechanisms viz., dynamic and static quenching (Moeiniafshari et al., 2015). The quenching mechanisms can be identified through examination of their quenching constant at different temperatures. If the quenching constant increases with temperature, it is called as dynamic quenching, whereas in static quenching, the quenching constant is inversely proportional to the temperatures (Reshma et al., 2018; Sun et al., 2013). To determine the quenching mechanism,

the fluorescence quenching data at 288, 298, and 310 K were further evaluated by utilizing supplementary equation 1. From the equation, the values of  $K_{sv}$  and  $k_q$  were shown in Fig. 2A and values are listed in Table 1. From the fig and table, it was seen that the values of  $K_{sv}$  increases with increasing temperature. The trends of  $K_{sv}$  with respect to temperatures indicated that the catechin and  $\beta$ -Lg interacted each other through dynamic quenching mechanism. The values of  $k_q$  were also calculated by applying supplementary equation 2. It was reported that the fluorescence lifetime of the biopolymer was around  $\sim 10^{-8}$  s (Wu et al., 2018). The values of  $K_q$  obtained from supplementary equation 2 are higher than the values of maximum scatter collision quenching constant ( $2 \times 10^{10}$  L mol<sup>-1</sup>s<sup>-1</sup>) of biomolecules alone. The increased value of  $K_q$  is supporting the fact that the mechanism of quenching between catechin and  $\beta$ -Lg was found to be dynamic type not a static type (Hu et al., 2006). The fluorescence quenching data were further analyzed by applying modified Stern–Volmer equation (supplementary equation 3) for the calculation of number of binding site and binding constant of  $\beta$ -Lg-catechin interaction. The plot of  $F_0/(F_0 - F)$  versus  $1/[\text{catechin}]$  (Fig. 2B) yields  $1/F_a$  as the intercept, and  $1/(F_a K_a)$  as the slope. The slope of modified graph gives the information about number of binding site and intercept provide information about binding constant. The number of binding site and binding constants are tabulated in table 1. The numbers of binding sites were calculated 0.9448, 1.0830 and 1.1132 at 288, 298 and 310 K. The  $K_a$  values of  $\beta$ -Lg-catechin system were got to be  $0.132 \times 10^{-5}$  L mol<sup>-1</sup> at 288 K;  $0.4810 \times 10^{-5}$  L mol<sup>-1</sup>, at 298 K;  $1.39 \times 10^{-5}$  L mol<sup>-1</sup> at 310 K (Table 1). The increasing values of  $K_a$  with increasing temperature are suggesting that the dynamic type of quenching was involved between  $\beta$ -Lg-catechin interactions.

#### 3.2. Examination of the binding forces involved between $\beta$ -Lg-catechin interactions:

The binding forces involved between  $\beta$ -Lg-catechin interactions were examined with the help of thermodynamic parameters. There are four main forces namely hydrogen bonds, van der Waals forces, hydrophobic, and electrostatic interactions involved between protein-ligand interaction. According to Ross and Subramanian research, it was proposed that if  $\Delta H > 0$ ,  $\Delta S > 0$ , hydrophobic interaction will be the main force; when  $\Delta H < 0$ ,  $\Delta S < 0$ , van der Waals forces and hydrogen bonds involved in the interaction; when  $\Delta H < 0$ ,  $\Delta S > 0$ , only electrostatic forces will involve (Ross and Subramanian 1981). The thermodynamic parameters of  $\beta$ -Lg-

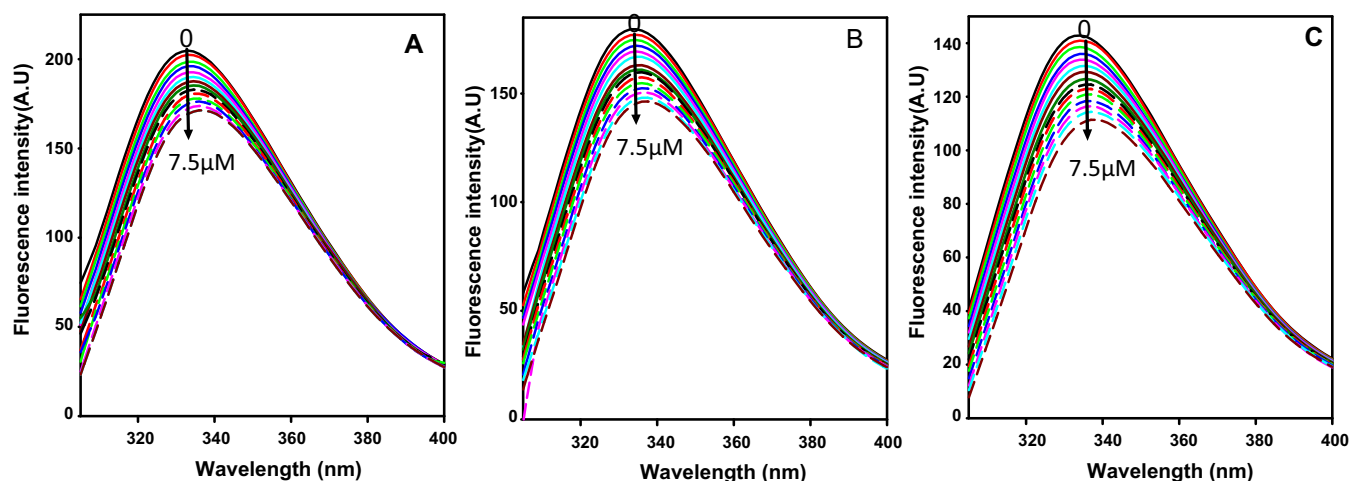
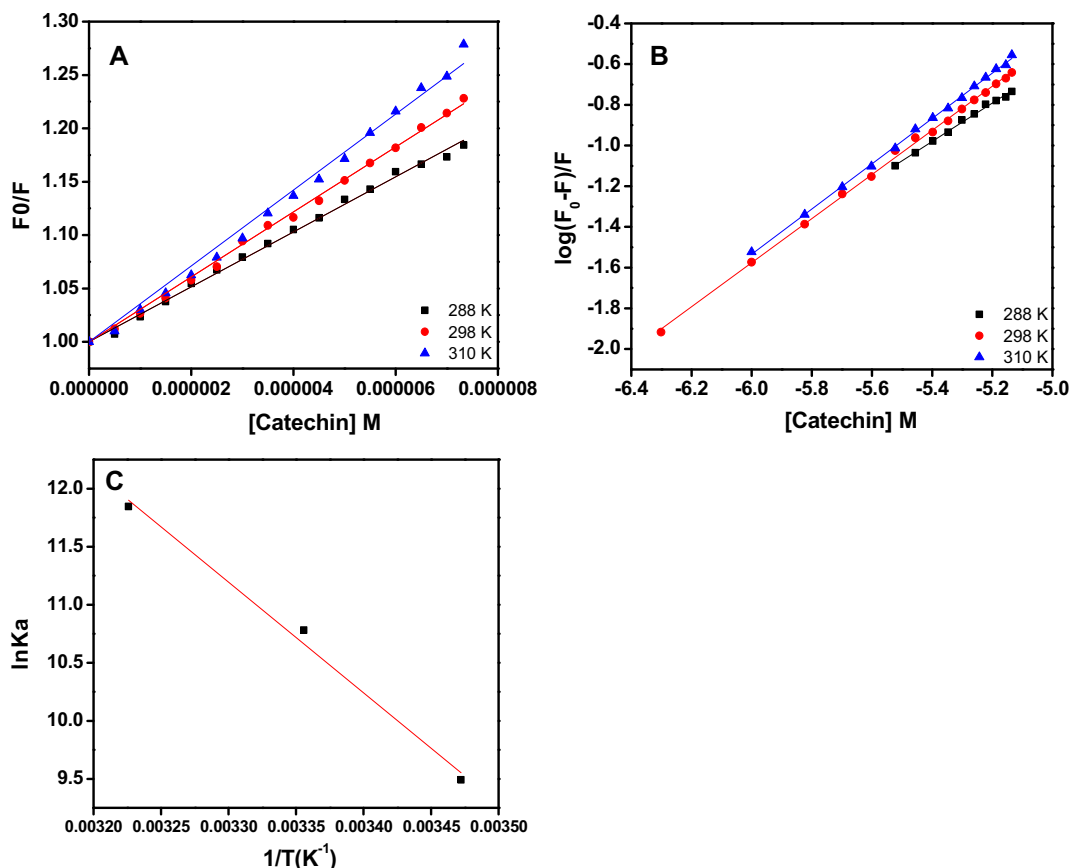


Fig. 1. Fluorescence quenching spectra of  $\beta$ -Lg (2.0  $\mu$ M) in presence of catechin (0–7.5  $\mu$ M) at 288 K (A), 298 K (B) and 310 K (C) at pH 7.4.



**Fig. 2.** Stern–Volmer (A) and modified Stern–Volmer ( $\log [(F_0-F)/F]$  versus  $\log [\text{catechin}]$ ) (B) and plot  $\ln K_a$  against  $1/T$  for interaction catechin with  $\beta$ -Lg at three different (288 K, 298 K and 310 K) temperatures.  $\beta$ -Lg was 2.0  $\mu\text{M}$  in every sample and excited at 295 nm.

**Table 1**

The spectroscopic parameters of  $\beta$ -Lg-catechin interaction at three different (288, 298 and 310 K) temperatures at physiological pH.

S.No.	T (K)	$K_{sv} \cdot 10^{-4}$ (L/mol)	$K_q \cdot 10^{12}$ (L/mol/s)	$R^2$	n	$K_A \cdot 10^{-5}$ (L/mol)
1	288	2.5	2.5	0.9966	0.9448	0.132
2	298	3.0	3.0	0.9977	1.0830	0.4810
3	310	3.5	3.5	0.9922	1.1132	1.39

catechin interactions were calculated from the van't Hoff equation (supplementary equation 4). The slope of the van't Hoff formula tells us about enthalpy change ( $\Delta H$ ). However, the free energy change ( $\Delta G$ ) is calculated from the supplementary equation no 5. The binding constants values at the three different temperatures, 288, 298 and 310 K were used to calculate the thermodynamic parameters and values are fitted in linear van't Hoff plot presented in Fig. 3 and in Table 2. The values are obtained after fitting the equation 4 and 5 and the data is presented in Table 2. As we can see from the Table 2, the obtained negative values of  $\Delta G$  are indicating that the interaction between  $\beta$ -Lg and catechin is spontaneous process. Moreover,  $\Delta H$  and  $\Delta S$  values were estimated to be positive, which designated that the hydrophobic interactions are mainly involved in the interaction between  $\beta$ -Lg and catechin. Similar observation was also found when carborane trimer 5 interacted with bovine serum albumin (Jena et al., 2019). The positive values of both  $\Delta H$  and  $\Delta S$  are suggest that the reaction between  $\beta$ -Lg and catechin was endothermic. The fluorescence quenching

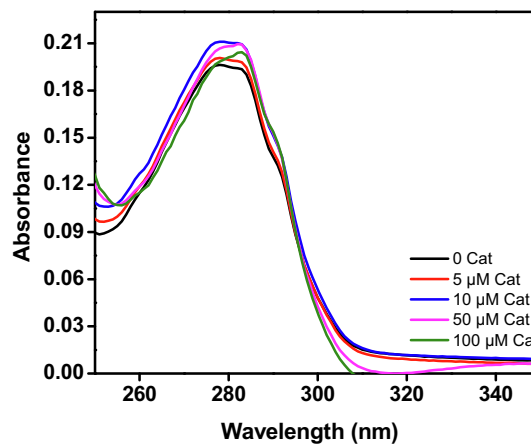


**Fig. 3.** UV–Vis absorption spectra of  $\beta$ -Lg (10.00  $\mu\text{M}$ ) without and with catechin (5.0, 10.0, 50.0 and 90.0  $\mu\text{M}$ ) at pH 7.4.

**Table 2**  
Thermodynamic parameters of binding of  $\beta$ -Lg: catechin at 288, 298 and 310 K.

S.No.	T (K)	$\Delta G$ (KJ/mol)	$\Delta H$ (KJ/mol)	$\Delta S$ (J/mol/K)
1	288	-52.33328		
2	298	-61.51569	79.22743	354.5173
3	310	-70.3071		

results at three different temperatures also suggest that the  $\beta$ -Lg-catechin interacted through hydrophobic interaction and its dynamic process of quenching. The reaction is spontaneous and endothermic.

### 3.3. UV-Vis absorption measurements:

The UV-Vis absorption spectroscopy is widely exploited to study the protein-drug complexation and protein conformational changes (Chi and Liu, 2010). This technique is dependent on degree of absorption of UV-vis light by the protein molecule. The absorption of UV light occurs due to the presence of aromatic amino acids mostly tryptophan, tyrosine and phenylalanine. The absorbance of tryptophan, tyrosine and phenylalanine depends on the microenvironment of their chromophores, and their wavelength shift either red or blue depends upon the polarity of surrounding environment (Pathak et al., 2016). We have collected the absorption spectra  $\beta$ -Lg without as well as with catechin (5 and 100  $\mu$ M) as shown in Fig. 3. Absorption spectrum of  $\beta$ -Lg alone shows maximum absorption around 280 nm because all aromatic amino acids absorb light maximally at 280 nm. Upon addition of different concentrations of catechin, significant increase in the absorbance of  $\beta$ -Lg with red shift in the wavelength maxima was recorded. The increase in absorption and shift in wavelength maximum shows that there is complex formation between  $\beta$ -Lg and catechin and polarity of microenvironment is also changed. It is also reported that the mechanism behind increase in absorption and shift in wavelength maximum towards higher wavelength is due to the exposure of aromatic amino acids to the external environment (Alam et al., 2015).

### 3.4. Secondary structure modification upon catechin binding with $\beta$ -Lg:

Circular dichroism (CD) spectroscopy is frequently employed to access the changes or modifications in protein's secondary as well as tertiary structure (Khan et al., 2019). The far-UV and near-UV CD spectra give information about protein's secondary and tertiary structure, respectively. The shape of far-UV CD spectra indicates the content of secondary structure ( $\alpha$ -helix,  $\beta$ -sheet and random coil). The  $\alpha$ -helical rich protein has two minima (208 and 222 nm),  $\beta$ -sheet has one minima (218 nm) and random coil protein have only one minima at 200 nm. The far-UV spectral curve of  $\beta$ -Lg without and with catechin in the sodium phosphate buffer, at room temperature, is shown in Fig. 4.  $\beta$ -Lg alone curve contained one negative band around ~218 nm, which was typical features of the  $\beta$ -class of proteins such as other  $\beta$ -sheeted protein already reported (Ismail et al., 2018). The far-UV CD spectra of  $\beta$ -Lg with 0, 10, 50 and 100  $\mu$ M of catechin was shown in Fig. 4. It can be seen from the fig., the negative ellipticity of  $\beta$ -Lg in the presence of 10, 50 and 100  $\mu$ M catechin was slightly increased with 2–3 nm red shifts. The increase in negative ellipticity with slight red shift of wavelength is indicated that the secondary structure of  $\beta$ -Lg modified due to catechin binding.

### 3.5. Analysis of molecular docking

The docking protocol adopted in this study was validated by redocking the ligand (tetracaine) which was bound in the X-ray crys-

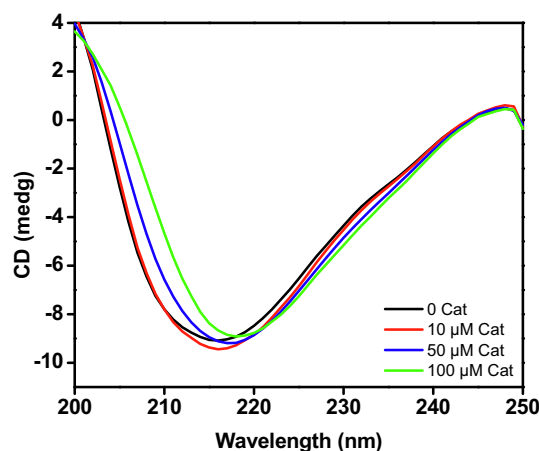


**Fig. 4.** Far-UV CD spectra of native  $\beta$ -Lg (5.0  $\mu$ M) in the presence of different concentrations of catechin (5.0, 10.0, 50.0 and 100.0  $\mu$ M) at pH 7.4.

tal structure of  $\beta$ -Lg. The docked and X-ray crystal poses of ligand were superimposed and their root mean square deviation (RMSD) was calculated. We found that the RMSD of ligand bound to  $\beta$ -Lg was 1.0201 Å (Supplementary fig. S1). Since, the observed RMSD was lower than the prescribed upper limit of 2 Å, we assumed that the docking procedure employed here was accurate.

Our results indicated that catechin binds strongly at the central cavity of  $\beta$ -Lg (Fig. 5A). The  $\beta$ -Lg-catechin complex was principally stabilized by hydrophobic interactions with amino acid residues such as Pro38, Leu39, Val41, Val43, Ile56, Leu58, Ile71, Ile84, Val92, Phe105 and Met107. Moreover, polar amino acid residue (Asn90) along with charged residues such as Lys60, Glu62 and Lys69 were also involved in  $\beta$ -Lg-catechin interaction (Fig. 5B). Further, the docking energy (XP score) and the corresponding docking affinity of catechin towards  $\beta$ -Lg were estimated as  $-6.824$  kcal mol<sup>-1</sup> and  $1.01 \times 10^5$  M<sup>-1</sup> respectively (Table 3). Glide e-model score and MM-GBSA of catechin bound to  $\beta$ -Lg were estimated to be  $-35.702$  and  $-61.735$  kcal mol<sup>-1</sup> respectively (Table 3).

The molecular docking of control ligand (i.e. the inhibitor bound to protein in the X-ray structure i.e. tetracaine) with the  $\beta$ -Lg revealed that tetracaine binds at the central cavity (Supplementary fig. S2A) and the complex was stabilized by a network of hydrophobic interaction with Ile12, Val15, Pro38, Leu39, Val41, Val43, Leu46, Leu54, Ile56, Leu58, Ile71, Ile84, Val92, Val94, Leu103, Phe105, Met107 and Leu122. Other amino acid residues involved in  $\beta$ -Lg-tetracaine interactions were Lys60, Lys69 and Asn90 (Supplementary fig. S2B). The amino acid residues of  $\beta$ -Lg interacting with tetracaine such as Pro38, Leu39, Val41, Val43, Ile56, Leu58, Ile71, Ile84 and Val92 have been found to also interact with catechin. Moreover, the docking energy and the corresponding docking affinity of tetracaine towards  $\beta$ -Lg were estimated as  $-6.963$  kcal mol<sup>-1</sup> and  $4.27 \times 10^6$  M<sup>-1</sup> respectively (Table 3). Glide e-model score and MM-GBSA of tetracaine bound to  $\beta$ -Lg were estimated to be  $-45.702$  and  $-83.021$  kcal mol<sup>-1</sup> respectively (Table 3).

### 3.6. Analysis of molecular dynamics simulation

The stability of  $\beta$ -Lg-catechin complex was evaluated by performing molecular dynamics simulation for 50 ns at 300 K. Fig. 6A shows the RMSDs of  $\beta$ -Lg C $\alpha$ -atoms without and with catechin. The RMSD of a protein gives the information about structural conformation for the entire period of simulation. The analysis of RMSD indicates if the simulation has equilibrated or

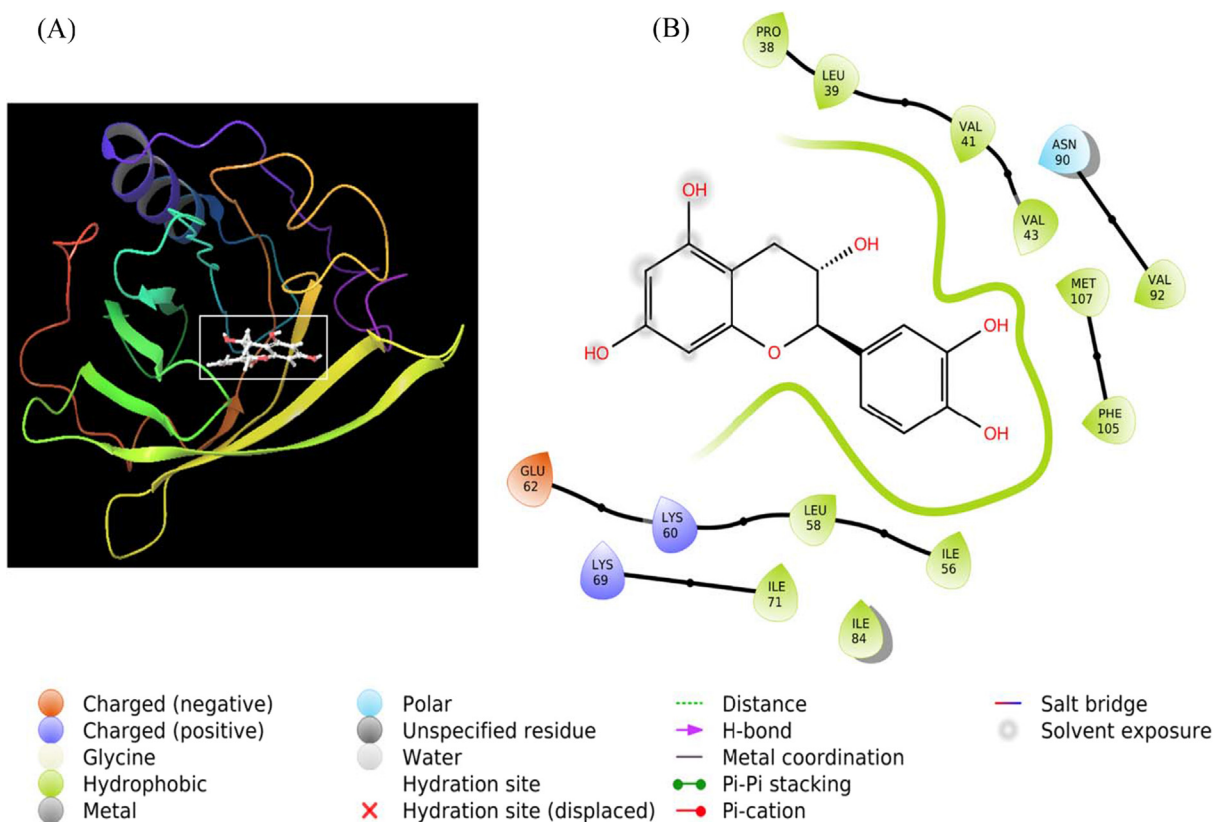


**Fig. 5.** Molecular docking of catechin with  $\beta$ -Lg. (A) Binding of catechin at the central cavity of  $\beta$ -Lg, and (B) Various interactions and amino acid residues involved in stabilizing catechin- $\beta$ -Lg complex.

**Table 3**  
Molecular docking parameters for  $\beta$ -Lg-catechin interaction.

Ligands	Hydrophobic residues	Other residues	Docking score (kcal mol <sup>-1</sup> )	Glide e-model (kcal mol <sup>-1</sup> )	MM-GBSA <sup>#</sup> (kcal mol <sup>-1</sup> )	Docking affinity (M <sup>-1</sup> )
Tetracaine (Control)	Ile12, Val15, <b>Pro38, Leu39, Val41, Val43</b> , Leu46, Leu54, <b>Ile56, Leu58, Ile71, Ile84, Val92</b> , Val94, Leu103, <b>Phe105, Met107</b> , Leu122	<b>Lys60, Lys69, Asn90</b>	-6.963	-45.702	-83.021	$1.28 \times 10^5$
Catechin	<b>Pro38, Leu39, Val41, Val43, Ile56, Leu58, Ile71, Ile84, Val92, Phe105, Met107</b>	<b>Lys60, Glu62, Lys69, Asn90</b>	-6.824	-35.702	-61.735	$1.01 \times 10^5$

The residues shown in BOLD represents that these were commonly involved in the interaction with Tetracaine (control) and Catechin.

<sup>#</sup> Molecular docking parameters for  $\beta$ -Lg-catechin interaction.

not. For a properly equilibrated and stable system, the fluctuations towards the end of the simulation should be within 1–3 Å for a globular proteins. Changes higher than that, however, suggest that the protein is undergoing a large conformational change during the simulation. In this work, the RMSD values of  $\beta$ -Lg were fluctuating around  $\sim 1.15$  Å, implying a stable confirmation of the protein. Further, the RMSD of protein in the presence of catechin indicates that it was stabilized after initial variations for the first 10 ns; however, it was much lower than the acceptable limit of 2 Å (Fig. 6A). Similarly, the RMSD value of catechin alone remains constant around 0.53 Å. The analysis of RMSD values indicate that catechin binds at the active site of  $\beta$ -Lg and the  $\beta$ -Lg-catechin complex is stable. The formation of a stable  $\beta$ -Lg-catechin complex was also suggested by observing the changes in various surface areas such as molecular surface area (MolSA), polar surface area (PSA), and solvent accessible surface area (SASA) of  $\beta$ -Lg-catechin complex as a

function of simulation time. We observed that MolSA, PSA and SASA remained persistent within the prescribed limits, thus confirming a stable complex between  $\beta$ -Lg and catechin (Fig. 6B). Furthermore, the radius of gyration (rGyr) of catechin remains constant over the simulation time, thereby signifying a compact structure of catechin (Fig. 6C).

The local conformational changes along  $\beta$ -Lg chain were probed by analyzing the root mean square fluctuation (RMSF) with respect to simulation time (Fig. 6D). The areas of  $\beta$ -Lg which fluctuate the most during simulation are indicated in blue. It is clear that the loop regions (indicated by the white bar) fluctuate the most during simulation. Conversely, alpha-helices and beta-sheets as represented by blue and pink bars were rigid. It is noteworthy that the RMSF of  $\beta$ -Lg corresponds with the X-ray B-factor. Furthermore, the vertical green lines on the X-axis show the interaction between  $\beta$ -Lg and catechin.

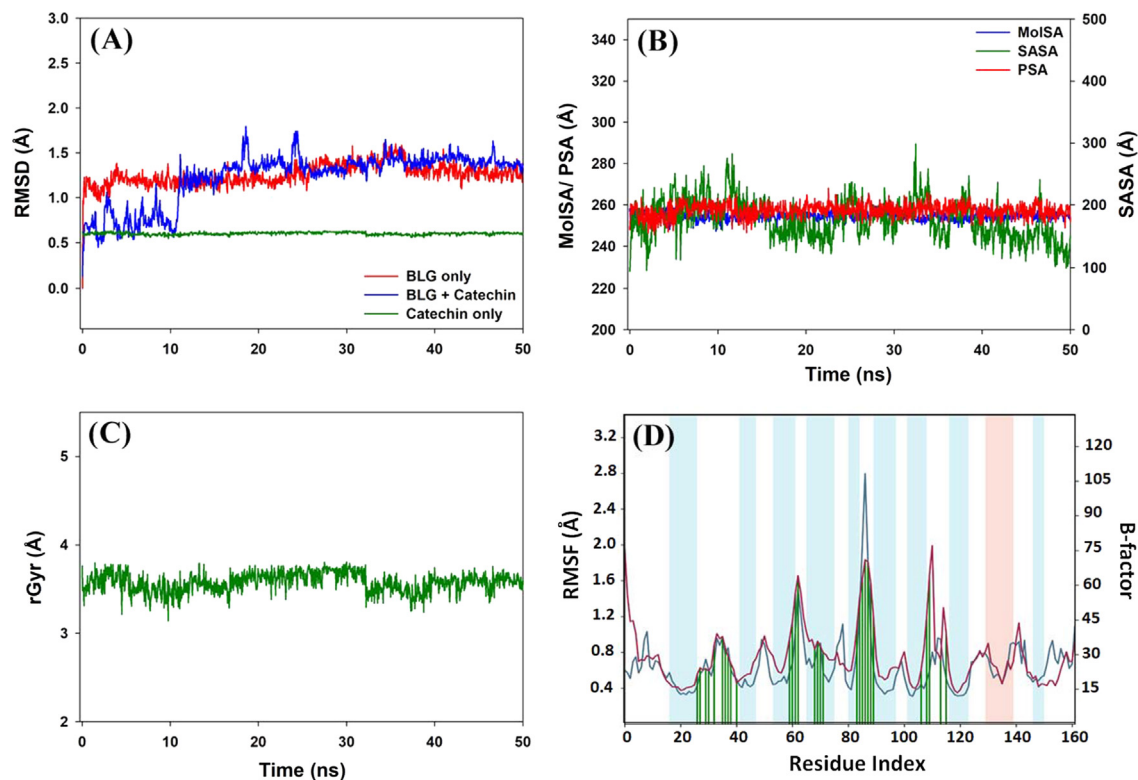


**Fig. 6.** Characterization of  $\beta$ -Lg-catechin interaction parameters as a function of molecular dynamics simulation time. (A) RMSD of  $\beta$ -Lg C $\alpha$ -atoms in the absence and presence of catechin. (B) Dependence of various surface areas associated with  $\beta$ -Lg-catechin complex as, (C) Variation in radius of gyration (rGyr) of catechin, and (D) RMSF deviation of  $\beta$ -Lg and its correlation with experimentally determined X-ray B-factor. The point of contact of catechin with  $\beta$ -Lg residues is shown by vertical green lines on X-axis.

#### 4. Conclusions

In this work authors have provided several evidences about the mechanism of interaction of tea polyphenol “catechin” with milk protein  $\beta$ -Lg. Intrinsic fluorescence measurements established that catechin interacted with  $\beta$ -Lg and lower down (quenched) the fluorescence intensity and the mechanism of interaction is dynamic type. According to thermodynamic data obtained by intrinsic fluorescence, measurements at three different temperatures suggest that hydrophobic interaction is majorly involved in  $\beta$ -Lg-catechin interaction. The secondary as well as tertiary structure of  $\beta$ -Lg is also modified due  $\beta$ -Lg-catechin interaction. The analysis of molecular docking and molecular dynamics simulation confirms that catechin bind at the central cavity of  $\beta$ -Lg and hydrophobic interaction involved in the stabilization  $\beta$ -Lg-catechin complex.

#### Acknowledgement

The authors extend their appreciation to Deanship of Scientific Research, King Saud University for funding this work through Research Group no. RGP-1439-014.

#### Appendix A. Supplementary material

Supplementary data to this article can be found online at <https://doi.org/10.1016/j.jsps.2020.01.002>.

#### References

Nozaki, A., Kimura, T., Ito, H., Hatano, T., 2009. Interaction of phenolic metabolites with human serum albumin: A circular dichroism study. *Chem. Pharm. Bull.* 57, 1019–1023.

- Moeniafshari, A.A., Zarrabi, A., Bordbar, A.K., 2015. Exploring the interaction of naringenin with bovine beta-casein nanoparticles using spectroscopy. *Food Hydrocoll.* 51, 1–6.
- Jena, B.B., Satish, L., Mahanta, C.S., et al., 2019. Interaction of carborane-appended trimer with bovine serum albumin: A spectroscopic investigation. *Inorg. Chim. Acta.* 491, 52–58.
- Patel, B.K., Sepay, N., Mahapatra, A., 2019. Curious Results in the Prospective Binding Interactions of the Food Additive Tartrazine with  $\beta$ -Lactoglobulin. *Langmuir* 35 (35), 11579–11589.
- Qin, B.Y., Bewley, M.C., Creamer, L.K., et al., 1999. Functional implications of structural differences between variants A and B of bovine  $\beta$ -lactoglobulin. *Protein Sci.* 8, 75–83.
- Dufour, C., Dangles, O., 2005. Flavonoid-serum albumin complexation: determination of binding constants and binding sites by fluorescence spectroscopy. *Biochimica. et Biophysica. Acta* 1721, 164–173.
- Kanakis, C., Hasni, I., Bourassa, P., et al., 2011. Tajmir-Riahi, Milk  $\beta$ -lactoglobulin complexes with tea polyphenols. *Food Chem.* 127 (3), 1046–1055.
- Lange, D.C., Kothari, R., Patel, R.C., et al., 1998. Retinol and retinoic acid bind to a surface cleft in bovine b-lactoglobulin: a method of binding site determination using fluorescence resonance energy transfer. *Biophys. Chem.* 74, 45–51.
- Yadav, D.K., Kumar, S., Choi, E.H., et al., 2018a. Insight into the molecular dynamic simulation studies of reactive oxygen species in native skin membrane. *Front Pharmacol.* 9, 644.
- Yadav, D.K., Kumar, S., Saloni, et al., 2018b. Molecular Insights into the Interaction of RONS and Thieno[3,2-c]pyran analogs with SIRT6/COX-2: a molecular dynamics study. *Sci Rep.* 8 (1), 4777.
- Yadav, D.K., Rai, R., Kumar, N., et al., 2016. New arylated benzo[h]quinolines induce anti-cancer activity by oxidative stress-mediated DNA damage. *Sci. Rep.* 6, 38128.
- Du, G.J., Wang, C.Z., Qi, L.W., et al., 2013. The synergistic apoptotic interaction of panaxadiol and epigallocatechingallate in human colorectal cancer cells. *Phytother. Res.* 27 (2), 272–277.
- Shen, H., Gu, Z., Jian, K., Qi, J., 2013. In vitro study on the binding of gemcitabine to bovine serum albumin. *J. Pharm. Biomed. Anal.* 75, 86–93.
- Sun, H., Wu, Y., Xia, X., Shi, Z., 2013. Spectroscopic studies on the interaction characteristics between norethisterone and bovine serum albumin. *J. Lumin.* 134, 580–587.
- Wu, H., Chen, M., Shang, M., et al., 2018. Insights into the binding behavior of bovine serum albumin to black carbon nanoparticles and induced cytotoxicity. *Spectrochim. Acta A Mol. Biomol. Spectrosc.* 200, 51–57.
- Zhang, H., Yu, D.D., Sun, J., et al., 2014. Interaction of milk whey protein with common phenolic acids. *J. Mol. Struct.* 1058, 228e233.

- Monaco, H.L., Zanotti, G., Spadon, P., et al., 1987. Crystal structure of the trigonal form of bovine beta-lactoglobulin and of its complex with retinol at 2.5 Å resolution. *J. Mol. Biol.* 197, 695–706.
- Graham, H.N., 1992. Green tea composition, consumption, and polyphenol chemistry. *Prev. Med.* 21, 334–350.
- Arts, I.C.W., de Hollman, P.C.H., Mesquita, H.B.B., et al., 2001. Dietary catechins and epithelial cancer incidence: The Zutphen elderly study. *Int. J. Cancer.* 92, 298–302.
- Dreostic, I.E., Wargovich, M.J., Yang, C.S., 1997. Inhibition of carcinogenesis by tea: the evidence from experimental studies. *Crit. Rev. Food Sci. Nutr.* 37, 761–770.
- Jia, J., Gao, X., Hao, M., Tang, L., 2017. Comparison of binding interaction between beta-lactoglobulin and three common polyphenols using multi-spectroscopy and modeling methods. *Food Chem.* 228, 143–151.
- Loch, J.L., Bonarek, P., Polit, A., et al., 2015. Beta-Lactoglobulin interactions with local anaesthetic drugs - Crystallographic and calorimetric studies. *Int. J. Biol. Macromol.* 80, 87–94.
- Khan, J.M., Malik, A., Sen, P., et al., 2019. Different conformational states of hen egg white lysozyme formed by exposure to the surfactant of sodium dodecyl benzenesulfonate. *Int. J. Biol. Macromol.* 128, 54–60.
- Fengru, L., Yiyin, Z., Qiuyang, Y., et al., 2019. Exploration of the binding between ellagic acid, a potentially risky food additive, and bovine serum albumin. *Food Chem. Toxicol.* 134, 110867.
- Ragona, L., Fogolari, F., Zetta, L., et al., 2000. Bovine beta-lactoglobulin: interaction studies with palmitic acid. *Protein Sci.* 9 (7), 1347–1356.
- Creamer, L.K., 1995. Effect of sodium dodecyl sulfate and palmitic acid on the equilibrium unfolding of bovine beta-lactoglobulin. *Biochemistry* 34, 7170–7176.
- Naghma, K., Hasan, M., 2019. Tea Polyphenols in Promotion of Human Health. *Nutrients* 11 (1), 39.
- Pathak, M., Mishra, R., Agarwala, P.K., et al., 2016. Binding of ethyl pyruvate to bovine serum albumin: calorimetric, spectroscopic and molecular docking studies. *Thermochim. Acta* 633, 140–148.
- Stojadinovic, M., Radosavljevic, J., Ognjenovic, J., et al., 2013. Binding affinity between dietary polyphenols and beta-lactoglobulin negatively correlates with the protein susceptibility to digestion and total antioxidant activity of complexes formed. *Food Chem.* 136 (3), 1263–1271.
- Ismael, M.A., Khan, J.M., Malik, A., et al., 2018. Unraveling the molecular mechanism of the effects of sodium dodecyl sulfate, salts, and sugars on amyloid fibril formation in camel IgG. *Coll. Surf. B Biointerf.* 170, 430–437.
- AlAjmi, M.F., Rehman, M.T., Hussain, A., 2018a. Pharmacoinformatics approach for the identification of Polo-like kinase-1 inhibitors from natural sources as anti-cancer agents. *Int. J. Biol. Macromol.* 116, 173–181.
- AlAjmi, M.F., Alam, P., Rehman, M.T., et al., 2018b. Interspecies anticancer and antimicrobial activities of genus *Solanum* and estimation of rutin by validated UPLC-PDA method. *Evid. Based Complement Alternat. Med.* 6040815, 1–13.
- Almajano, M.P., Delgado, M.E., Gordon, M.H., 2007. Changes in the antioxidant properties of protein solutions in the presence of epigallocatechin gallate. *Food Chem.* 101 (1), 126e130.
- Rehman, M.T., AlAjmi, M.F., Hussain, A., 2019. High-throughput virtual screening and Molecular dynamics simulation identified ZINC84525623 a potential inhibitor of NDM-1. *Int. J. Mol. Sci.* 20, 819.
- Alanazi, M.M., Almezhia, A.A., Bakheit, A.H., et al., 2019. Mechanistic interaction study of 5,6-Dichloro-2-[2-(pyridin-2-yl) ethyl]isoindoline-1,3-dione with bovine serum albumin by spectroscopic and molecular docking approaches. *Saudi Pharma. J.* 27, 341–347.
- Al-Shabib, N.A., Khan, J.M., Malik, A., et al., 2018. Molecular insight into binding behavior of polyphenol (rutin) with beta lactoglobulin: Spectroscopic, molecular docking and MD simulation studies. *J. Mol. Liq.* 269, 511–520.
- Ross, P.D., Subramanian, S., 1981. Thermodynamics of protein association reactions: forces contributing to stability. *Biochemistry* 20 (11), 3096–3102.
- Alam, P., Chaturvedi, S.K., Anwar, T., et al., 2015. Biophysical and molecular docking insight into the interaction of cytosine beta-D arabinofuranoside with human serum albumin. *J. Lumin.* 164, 123–130.
- Reshma, S.K., Vaishnav, I., Karbhal, M.L., et al., 2018. Ghosh, Spectroscopic studies on in vitro molecular interaction of highly fluorescent carbon dots with different serum albumins. *J. Mol. Liq.* 255, 279–287.
- Chaudhuri, S., Chakraborty, S., Sengupta, P.K., 2011. Probing the interactions of hemoglobin with antioxidant flavonoids via fluorescence spectroscopy and molecular modeling studies. *Biophys. Chem.* 154 (1), 26–34.
- Kumar, S., Yadav, D.K., Choi, E.H., et al., 2018. Insight from Molecular dynamic simulation of reactive oxygen species in oxidized skin membrane. *Sci Rep.* 8 (1), 13271.
- Uhrinova, S., Smith, M.H., Jameson, G.B., et al., 2000. Structural changes accompanying pH-induced dissociation of the beta-lactoglobulin dimer. *Biochemistry* 39, 3565–3574.
- Tantimongkolwat, T., Prachayasittikul, S., Prachayasittikul, V., 2019. Unravelling the interaction mechanism between cloquinol and bovine serum albumin by multi-spectroscopic and molecular docking approaches. *Spectrochim. Acta A Mol. Biomol. Spectrosc.* 216, 25–34.
- Xu, Y.J., Dai, T.T., Li, T., et al., 2019. Investigation on the binding interaction between rice glutelin and epigallocatechin-3-gallate using spectroscopic and molecular docking simulation. *Spectrochim. Acta A Mol. Biomol. Spectrosc.* 217, 215–222.
- Wu, X., Dey, R., Wu, H.U.I., et al., 2013. Studies on the interaction of epigallocatechin-3-gallate from green tea with bovine beta-lactoglobulin by spectroscopic methods and docking. *Int. J. Dairy. Technol.* 66 (1), 7–13.
- Mao, X., Xiao, X., Chen, D., et al., 2019. Tea and its components prevent cancer: a review of the redox-related mechanism. *Int. J. Mol. Sci.* 20, 5249–.
- Hu, Y., Liu, Y., Zhao, R., et al., 2006. Spectroscopic studies on the interaction between methylene blue and bovine serum albumin. *J. Photochem. Photobiol.* 179, 324–329.
- Chi, Z., Liu, R., 2010. Phenotypic characterization of the binding of tetracycline to human serum albumin. *Biomacromolecules.* 12, 203–209.
- Shah, Z.A., Li, R.C., Ahmad, A.S., et al., 2010. The flavanol (–)-epicatechin prevents stroke damage through the Nrf2/HO1 pathway. *J. Cereb Blood Flow Metab.* 30, 1951–1961.